

## **Toward a Global 1/25° HYCOM Ocean Prediction System with Tides**

Eric P. Chassignet  
Center for Ocean-Atmospheric Prediction Studies  
Florida State University  
phone: (850) 644-4581 fax: (850) 644-4841 email: [echassignet@coaps.edu](mailto:echassignet@coaps.edu)

Award #: N00014-09-1-0587  
<http://www.hycom.org>

### **LONG-TERM GOALS**

The overall technical goal is to implement a 1/25° horizontal resolution global ocean prediction system based on the HYbrid Coordinate Ocean Model (HYCOM) with tides and dynamic sea ice. The scientific goals include but are not limited to a) evaluation of the internal tides representation in support of field programs, b) data assimilation in the presence of tides, c) evaluation of the model's ability to provide useful boundary conditions to high resolution coastal models, d) interaction of the open ocean with ice, e) shelf–deep ocean interactions, f) upper ocean physics including mixed layer/sonic depth representation, g) mixing, etc.

### **OBJECTIVES**

Perform the R&D necessary to develop, evaluate, and investigate the dynamics of 1/25° global HYCOM with tides coupled to CICE (the Los Alamos sea ice model) with atmospheric forcing only, with data assimilation via NCODA (NRL Coupled Ocean Data Assimilation), and in forecast mode. Work closely with NRL Stennis to incorporate advances in dynamics and physics from the science community into the HYCOM code maintained by the Navy.

### **APPROACH**

This past year, a series of HYCOM configurations is used to (b) investigate the interaction of the open ocean with ice, (b) evaluate the AMOC representation and (c) evaluate its performance under the CORE forcing. The current HYCOM development is the result of collaborative efforts among the Florida State University, University of Michigan, and the Naval Research Laboratory (NRL) as part of the multi-institutional HYCOM Consortium for Data-Assimilative Ocean Modeling (Bleck, 2002; Chassignet et al., 2003; Halliwell, 2004). This effort was initially funded by the National Ocean Partnership Program (NOPP) to develop and evaluate a data-assimilative hybrid isopycnal-sigma-pressure (generalized) coordinate ocean model (Chassignet et al., 2009). HYCOM has been configured globally and on basin scales at up to 1/25° (~3.5 km mid-latitude) resolution. More details on the latest simulations can be found at <http://www.hycom.org> and in the separate ONR reports on NRL activities by A. Wallcraft and the U. of Michigan activities by B. Arbic.

# Report Documentation Page

Form Approved  
OMB No. 0704-0188

Public reporting burden for the collection of information is estimated to average 1 hour per response, including the time for reviewing instructions, searching existing data sources, gathering and maintaining the data needed, and completing and reviewing the collection of information. Send comments regarding this burden estimate or any other aspect of this collection of information, including suggestions for reducing this burden, to Washington Headquarters Services, Directorate for Information Operations and Reports, 1215 Jefferson Davis Highway, Suite 1204, Arlington VA 22202-4302. Respondents should be aware that notwithstanding any other provision of law, no person shall be subject to a penalty for failing to comply with a collection of information if it does not display a currently valid OMB control number.

1. REPORT DATE <b>30 SEP 2013</b>		2. REPORT TYPE		3. DATES COVERED <b>00-00-2013 to 00-00-2013</b>	
4. TITLE AND SUBTITLE <b>Toward a Global 1/25 degrees HYCOM Ocean Prediction System with Tides</b>				5a. CONTRACT NUMBER	
				5b. GRANT NUMBER	
				5c. PROGRAM ELEMENT NUMBER	
6. AUTHOR(S)				5d. PROJECT NUMBER	
				5e. TASK NUMBER	
				5f. WORK UNIT NUMBER	
7. PERFORMING ORGANIZATION NAME(S) AND ADDRESS(ES) <b>Florida State University, Center for Ocean-Atmospheric Prediction Studies, 600 West College Avenue, Tallahassee, FL, 32306</b>				8. PERFORMING ORGANIZATION REPORT NUMBER	
9. SPONSORING/MONITORING AGENCY NAME(S) AND ADDRESS(ES)				10. SPONSOR/MONITOR'S ACRONYM(S)	
				11. SPONSOR/MONITOR'S REPORT NUMBER(S)	
12. DISTRIBUTION/AVAILABILITY STATEMENT <b>Approved for public release; distribution unlimited</b>					
13. SUPPLEMENTARY NOTES					
14. ABSTRACT					
15. SUBJECT TERMS					
16. SECURITY CLASSIFICATION OF:			17. LIMITATION OF ABSTRACT	18. NUMBER OF PAGES	19a. NAME OF RESPONSIBLE PERSON
a. REPORT <b>unclassified</b>	b. ABSTRACT <b>unclassified</b>	c. THIS PAGE <b>unclassified</b>			

## RESULTS

### Arctic Ocean

The Arctic Ocean model runs were performed with the HYbrid Coordinate Ocean Model (HYCOM) coupled with Los Alamos National Laboratory Community Ice Code (CICE). Two model configurations of the Arctic Ocean were used in the study: model with  $0.08^\circ$  (ARCc0.08) and with  $0.72^\circ$  (ARCc0.72) horizontal spacing (Fig.1). The vertical grid has 32 hybrid layers.

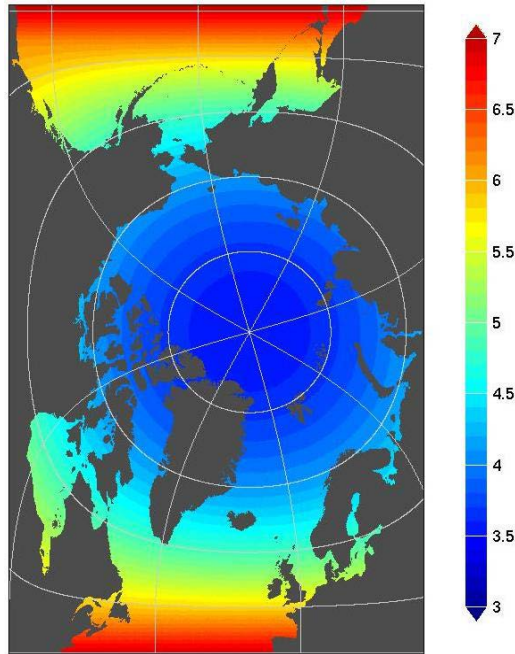


***Fig. 1. Model domain and horizontal resolution (km) of ARCc0.08.***

#### *High-latitude storms and water mass formation processes in the Nordic Seas*

The Nordic Seas (Greenland, Norwegian, Iceland, and Barents Seas) is a key region for maintenance of the Arctic Ocean thermohaline structure. This is the region of intense water mass formation through cooling, brine rejection, and mixing of Arctic Ocean and Atlantic waters. Misrepresentation of these processes in the ocean models will eventually result in biases of thermohaline structure of the Arctic Ocean. Ocean processes involved in the water mass formation in that area are largely controlled by surface winds. The most energetic winds in the Nordic Seas are associated with storms or cyclones. There are two major categories of cyclones in that region: the large-scale and meso-scale low-pressure systems. Meso- and small-scale cyclones are low-pressure systems with spatial scales in  $O(<10^3 \text{ km})$  and time scales from several hours to days. A subtype of this class of cyclones is Polar Low. These lows are very intense maritime low-pressure system with strong near-surface winds. Polar Lows form over the sea and predominantly during the winter months. The small-scale cyclones are difficult to observe due to their short life cycle and small size. It is speculated that the role of the meso-scale low-pressure systems in ocean processes is as large as that of the large-scale cyclones, mostly due to their higher frequency and stronger winds. Meso- and small-scale cyclones over the Arctic Ocean are poorly represented in the available observational reanalysis data. The following wind products are analyzed in

this study: Cross-Calibrated Multi-Platform surface wind data (CCMP); the NCEP/NCAR Reanalysis 2 (NCEPR); NCEP Climate Forecast System Reanalysis (CFSR); and Arctic System Reanalysis (ASR). Analysis of the wind products revealed that meso-scale features were not represented in either of the wind. Even large-scale storms have different representation in the wind products (Fig. 3). A suite of model experiments forced by different winds was conducted for 2005-2006.

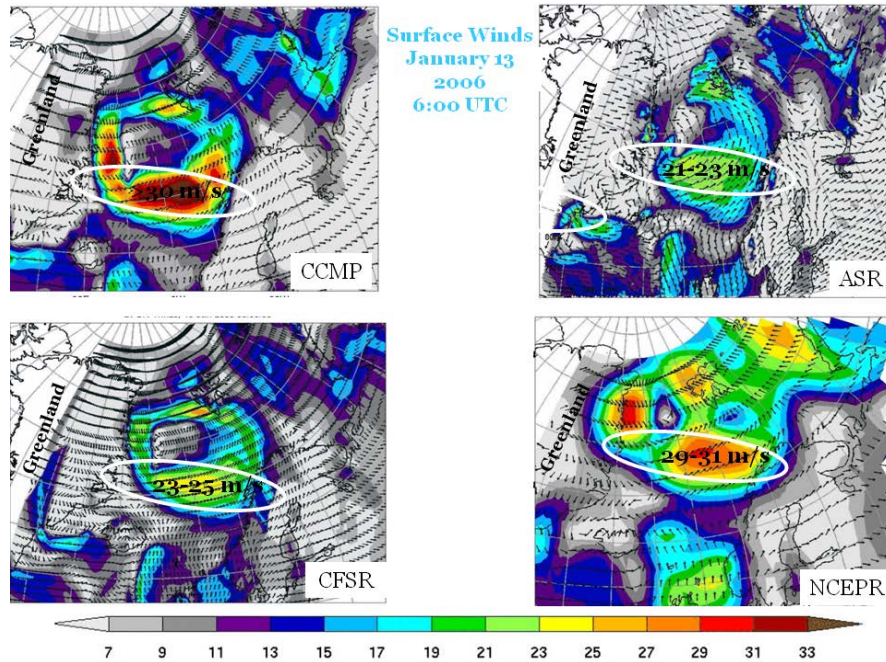


**Fig. 3. Different representation of the large-scale cyclone over the Greenland Sea in the wind products. Note the difference in the maximum winds.**

We find that

1. Different wind products have obviously different representation of storms in high latitudes (Fig. 3). This impacts all wind-driven process in the Arctic.
2. The upper-ocean currents from the model experiments forced by different winds differ in magnitude and direction (Fig. 4).
3. The air-sea fluxes are substantially different under the storms in the simulations driven by different winds (Fig. 5).
4. Discrepancies in the momentum and heat fluxes provided by different winds to the ocean impact the water mass formation processes in the model (Fig. 6).

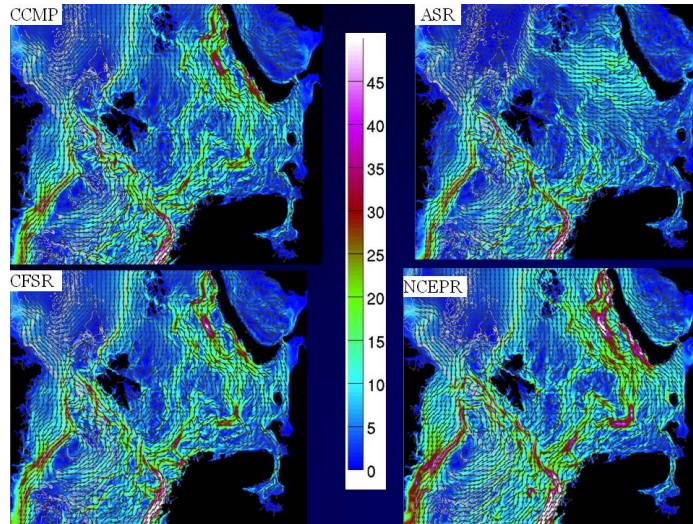


**Fig. 4.** Winter mean upper-ocean circulation in the Nordic Seas from the ARCC0.08 simulation.

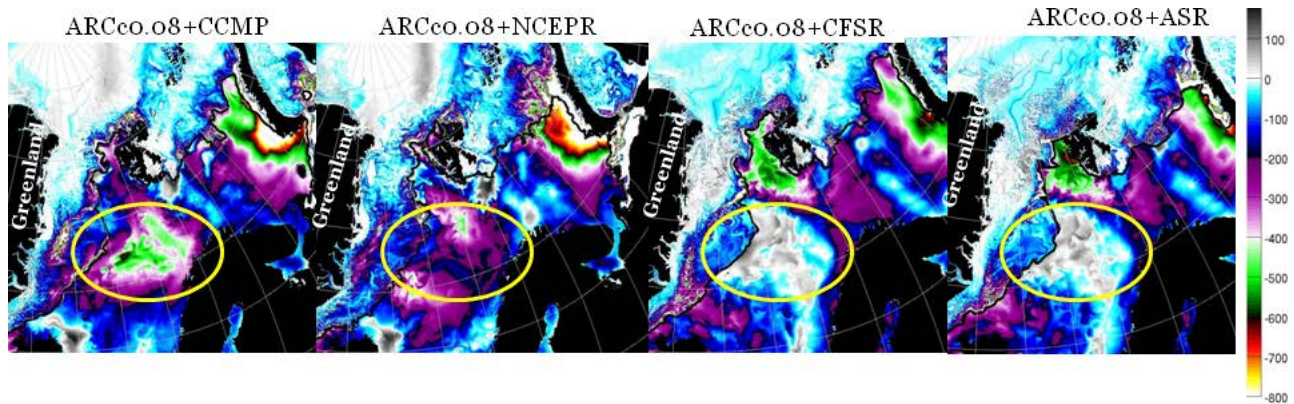


**Fig. 5.** Instantaneous net surface heat fluxes ( $W/m^2$ ) during storm shown in Fig. 3 in the simulations forced by winds from different products (indicated in the titles).

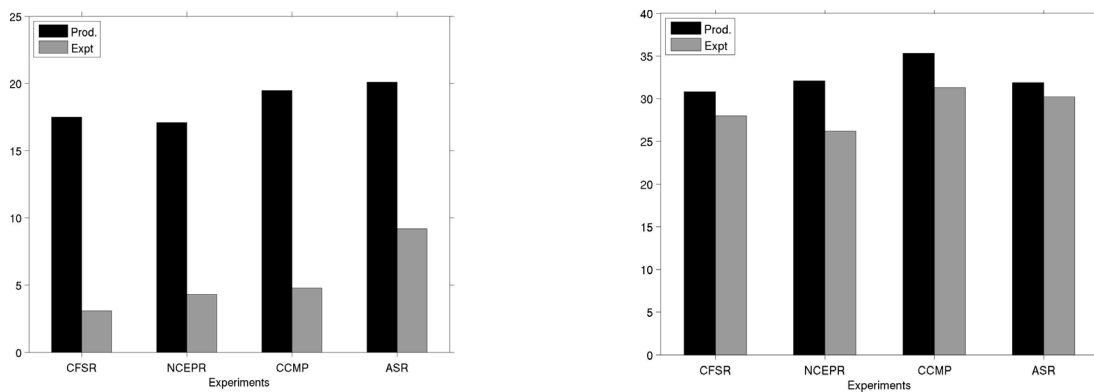


**Fig. 6.** Integrated dense water production (black bars) and export (gray) out of the Barents Sea (left) and Greenland Sea (right) in the simulations driven by different winds (horizontal axis).

### *Freshwater pathways in the Nordic Seas*

The Nordic Seas are a region of deep water formation. Deep waters formed in the convection regions constitute a component of the Meridional Overturning Circulation. Several studies relate intensity of deep convection in the Nordic Seas to freshwater content of the East Greenland Current arguing that a substantial fraction of this freshwater is supplied to convection regions. However, the actual pathways of freshwater from the East Greenland Current to the convection regions are not well known. Of particular interest is the fate of freshwater flux from Greenland which has substantially increased over the last decade. Can this freshwater propagate to deep convection regions? This study employs ARCc0.08 and ARCc0.72 to study freshwater pathways with origins in the East Greenland Current. Model experiments are used to analyze the role of wind forcing in the upper ocean circulation and propagation of freshwater in the region.

To date, a control run (with no Greenland rivers) has been performed for 2006 with (30-day) and “without” (4-year relaxation time scale) sea surface salinity relaxation. A second set of experiments has been run with monthly high-resolution Greenland runoff incorporated into the model. The runoff data are provided by J. Bamber for 1999 – present time period. Test experiments with and without SSS relaxation have been conducted for 2006. Model results are under analysis. It is noteworthy that for the experiments with Greenland Runoff, changes have been done to the HYCOM code to allow river water to be distributed under the sea ice.

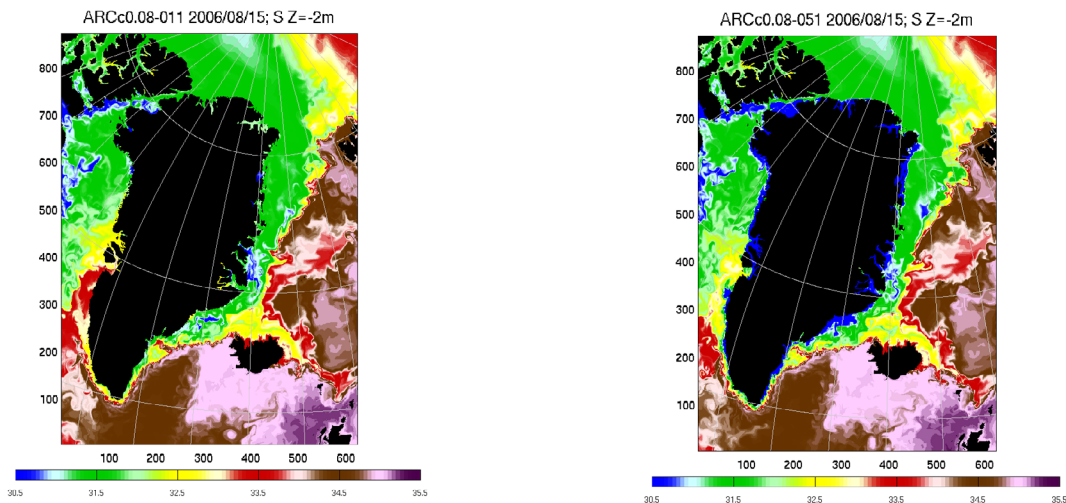


**Fig. 7. Snapshots of the upper ocean salinity field around Greenland on August 15, 2006 from the ARCc0.08 simulation without (left) and with (right) Greenland Runoff. The simulation is with 4-year relaxation time scale.**

### *Relation of current Arctic climate change to freshwater flux to the Nordic Seas*

One of the most intriguing manifestations of observed climate change is the cessation of decadal Arctic climate variability in the 21st century. Between 1950 and 1996, the Arctic atmospheric and oceanic circulation alternated between anticyclonic and cyclonic circulation regimes at 5 to 7 year intervals. Since 1997, however, the Arctic system has been dominated by a 16-year anticyclonic regime with environmental parameters that are atypical for anticyclonic climate state. In the 20th century, freshwater and heat exchange between the Arctic Ocean and the Nordic Seas were self-regulated and their interactions were realized via decadal climate auto-oscillations. It is hypothesized

that in the 21st century, these regular oscillations have been interrupted as a result of additional freshwater fluxes from Greenland. The excess freshwater from Greenland reduces deep convection in the northern seas, resulting in the cessation of decadal Arctic climate oscillations. Analyzing NAO index and air temperature (65-90°N) time series we have found that decadal changes in the Arctic were absent during Arctic warming in the 1920s – 1950s when Greenland ice melting was increased. Model experiments with different freshwater fluxes to the Nordic Seas (described above) are currently used to investigate this hypothesis.

## **AMOC Variability**

The state-of-the-art approach to measuring the Atlantic Meridional Overturning Circulation (AMOC) is to continuously observe the currents and hydrographic fields with a long-term, moored instruments array, to obtain the temporal mean value of the AMOC as well as the information on its time scale and range of the variability. For this purpose, the joint U.K.-U.S. Rapid Climate Change-MOC program (RAPID, hereafter) have instrumented a complete transbasin section along 26.5°N. Daily mean AMOC transport and its vertical structure have been derived from the RAPID data since April 2004 (e.g., Cunningham et al., 2007; Kanzow et al., 2007, 2010; Johns et al., 2008, 2011; Rayner et al., 2011; McCarthy et al., 2012). The RAPID results show that the AMOC is not slowly varying, as previously thought, but rather has a high variability on intraseasonal to seasonal time scales. In addition, there is significant variability on interannual and longer time scales. One question that arises is as to whether, or to what extent, the variability is coherent across different latitudes, so that the variability observed at one latitude is representative of a larger scale change (Willis, 2010). This question can be addressed using a high horizontal ocean model as long the model adequately represents the basic features of AMOC variability.

Results from two eddy-resolving HYCOM numerical simulations are presented here. The two simulations, one Atlantic, the other global, have several key features in common. Both have a horizontal resolution of 1/12°. Both were initialized using potential temperature (T) and salinity (S) from the ocean climatology, the Generalized Digital Environmental Model [GDEM, Carnes, 2009], and were spun-up from rest using the climatological surface forcing from the ECMWF reanalysis ERA40 [Uppala et al., 2005]. After spin-up (10 years for the global model and 15 years for the Atlantic), both use the 3-hourly, 0.5° Navy Operational Global Atmospheric Prediction System (NOGAPS, Rosmond et al., 2002). The global simulation covers 2003-2012, the Atlantic simulation covers 2004-2012. As a subset of the global model, the Atlantic model domain extends meridionally from 28°S to the Fram Strait at 80°N. No inflow or outflow is prescribed at the northern and southern boundaries. Within a buffer zone of about 3° from the northern and southern boundaries, the 3-D model T, S, and depth of isopycnal interface are restored to the monthly GDEM with an e-folding time of 5-60 days that increases with distance from the boundary. Vertically, the Atlantic simulation has the conventional 32 layers whereas the global model has 41 layers. The additional nine layers are all near the surface to resolve the seasonal thermocline in other parts of the global ocean. The Atlantic model, with different reference densities near bottom, uses some of the nonexistent bottom layers in the global model and has a finer vertical resolution in the deep Atlantic Ocean. This change, as documented in Xu et al. (2012), improves the vertical structure of the AMOC. The global simulation, which includes a coupled sea-ice model, instead of the simple energy loan sea-ice parameterization in the Atlantic simulation, shows improved water property (salinity in particular) in the upper layers of the Labrador Sea. However, the southward flow of NADW in the global simulation has significantly less

contribution from the Nordic Seas overflow water (NSOW), probably because of inadequate representation of the model water property in the Nordic Seas.

We employed an adaptive and temporally local decomposition method to separate the transport time series into variability modes of different time scale. The results show that at 26.5°N, our simulations yield most of the observed AMOC variability on intraseasonal, seasonal, and interannual time scales. The variability of the Florida Current transport in the Atlantic model also agrees reasonably well with the observations. Near 41°N, our model results represent well the observed variability on seasonal time scales, but is less successful on interannual time scales. On a long time scale, the observed AMOC transports at 26.5°N declined about 3 Sv from 2004 to 2012. The Atlantic model does not simulate this long-term change, but the global model does. Thus, the change may represent large-scale dynamics beyond the Atlantic model domain. Overall, the variability of the monthly mean AMOC transport in both the global and the Atlantic simulations is lower than the observations. The variability of the AMOC transport in the two simulations is very similar, despite differences in the model domain and the vertical structure of the southward limb. This indicates that most of the interannual and shorter term variability in our models is not induced by dense water formation to the north, or by the dynamics to the south of Atlantic model domain. The variability more likely is induced via the same atmospheric forcing used in two simulations, particularly the wind. This is in accord with recent works of Zhao and Johns (manuscript submitted to JPO; 2013 AMOC meeting presentation) and Yang (2013 AMOC meeting poster). They show that, in idealized two-layer models that contain no time mean AMOC, seasonal and interannual variability of the AMOC transport is induced by variation of the wind-driven subtropical gyre. Also, Ekman transports directly contribute to the AMOC variability on various time scales, such as the abnormally low AMOC transport in Winter 2009/2010 caused by the very low North Atlantic Oscillation (Xu et al., 2012; Hakkinen and Rhines, 2013). The notion of wind as the primary source of AMOC variability, at least within interannual time scales, highlights the need for better quantifying of the wind field and better understanding of the wind-driven ocean responses. When AMOC variability at different latitudes is considered, the results show little meridional coherence on an intraseasonal time scale, although large intraseasonal variations sometimes extend over long distances meridionally. The seasonal variability of the AMOC is connected from the subtropical to the subpolar North Atlantic, but is clearly separated from the subtropics to the tropics.

For the well-documented low transport at 26.5°N during the winter of 2009/2010, there is an opposite response in the subpolar North Atlantic. All the northward AMOC transports in the North Atlantic come from the South Atlantic. The model results show that the AMOC varies dramatically on seasonal time scales when crossing the tropical Atlantic. This seasonal variation is primarily due to Ekman transport near the surface, but is compensated to a small part by contribution of AAIW below the thermocline (Fig. 8). The importance of the Ekman transport in the tropical Atlantic is highlighted further in heat transport: At 10°N, the Ekman transport explains nearly all the northward heat flux. Horizontally, the circulation pattern in the upper layer of the tropics also change significantly in association with the seasonal AMOC variation. Particularly interesting, in August the NECC gains transport from the north as it flows eastward and recirculates south and westward to form a semiclosed gyre. This pattern differs from the classical picture of near-surface circulation in the tropical Atlantic by Richardson and Walsh (1986), but explains the slightly southward net transport in August. These results emphasize the value of eddy-resolving simulations in providing a detailed spatial structure of the circulation in addition to transbasin volume and heat transport estimates.



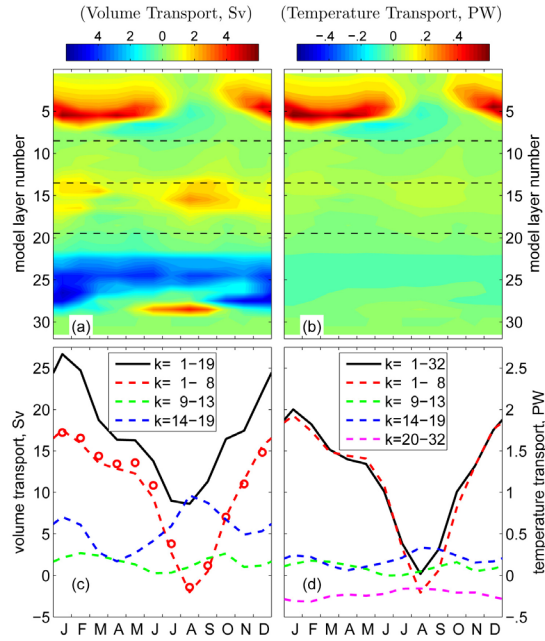


**Fig. 8: Monthly mean transports of volume (a, c) and temperature (b, d) across  $10^{\circ}\text{N}$  as a function of model layers. Circles in panel (c) denote the Ekman transport determined from model wind stress. Results are based on a 9-year mean of a  $1/12^{\circ}$  Atlantic simulation in 2004-2012.**

## CORE experiments

The aim of the Coordinated Ocean-ice Reference Experiments (CORE) is to compare results from several ocean-ice model using the same atmospheric forcing to create a basis that could be used to provide a mechanistic understanding of the role of the ocean in the climate system and to better quantify the importance of numerical choices. HYCOM, coupled with the Los Alamos CICE, was set-up following the CORE\_v2 protocol. The protocol consists of:

- an interannually varying atmospheric forcing (corresponding to the period 1948-2007) from Large and Yeager (2009) for 5 consecutive cycles.
- an SSS-relaxation corresponding to 4years/50m
- a surface salinity global normalization

The HYCOM-CICE global configuration uses version 2.2.74 of HYCOM and version 4.0 of CICE. It has a  $500 \times 382$  points tripolar grid of  $\sim 0.72^{\circ}$  resolution and 32 sigma-2 hybrid vertical layers. The sea-ice model provides the ocean model with ice-ocean stress, SST and ice cover. The ocean-ice fluxes are calculated using the energy loan ice model built in HYCOM. The initial conditions and the surface salinity climatology is the General Digital Environmental Model (GDEM4; Carnes et al., 2010) and the turbulent air-sea fluxes are computed using the Kara bulk formulae (Kara et al., 2004). To account for the temperature bias generated by this particular bulk formulation, a constant flux offset of  $\sim -10\text{W}$  is applied everywhere. To evaluate the sensitivity to the surface salinity relaxation, two experiments were performed: 1) we apply a 30days/50m SSS relaxation (SSS30d) and 2) we apply 4years/50m SSS

relaxation (SSS4y). In both cases, a surface salinity global normalization is also applied (i.e. no net salt flux). The model is first run 30 years (1948-1978) to evaluate each experiment's performance.

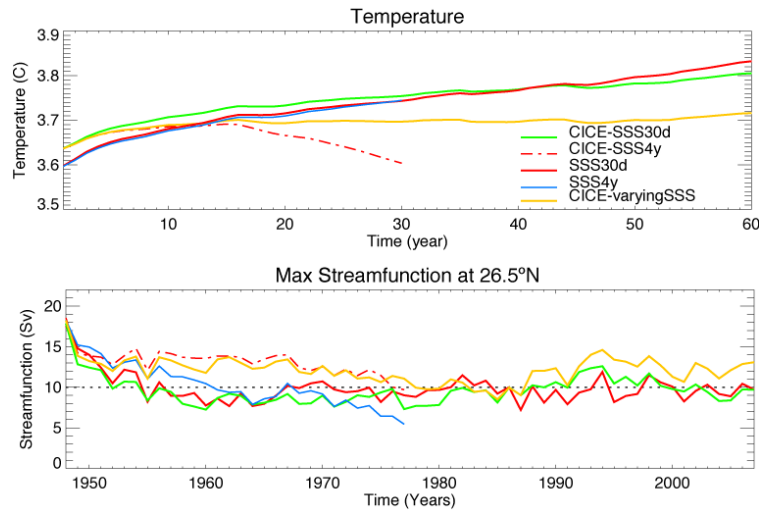


**Fig. 9. Evolution of the global temperature (top) and maximum of the AMOC (Sv; bottom) at 26.5°N for SSS30d (red), SSS4y (blue), CICE-SSS30d (green), CICE-SSS4y (dashed-red) and CICE-varyingSSS (yellow).**

Both experiments exhibit a similar increase of the global temperature ( $\sim 0.15^\circ\text{C}$ , Fig. 9 top) and SSH ( $\sim 9\text{cm}$ , not shown) after 30 years. A strong fresh bias is observed in SSS4y in the southern Ocean and the Arctic Ocean (Fig. 10, right). This fresh bias in the Arctic then partly feeds the subpolar gyre in SSS4y resulting in a continually decreasing Atlantic Meridional Overturning Circulation (AMOC) from 17 Sv at the beginning to 5 Sv after 30 years (Fig 9, bottom). In SSS30d, the surface salinity relaxation prevents these polar fresh biases, keeping the SSS of the supolar close to the climatology (Fig. 10, left). Consequently, while we still do observe a decrease of the AMOC in SSS30d, it stabilizes close to  $\sim 9$  Sv after 10-15 years.

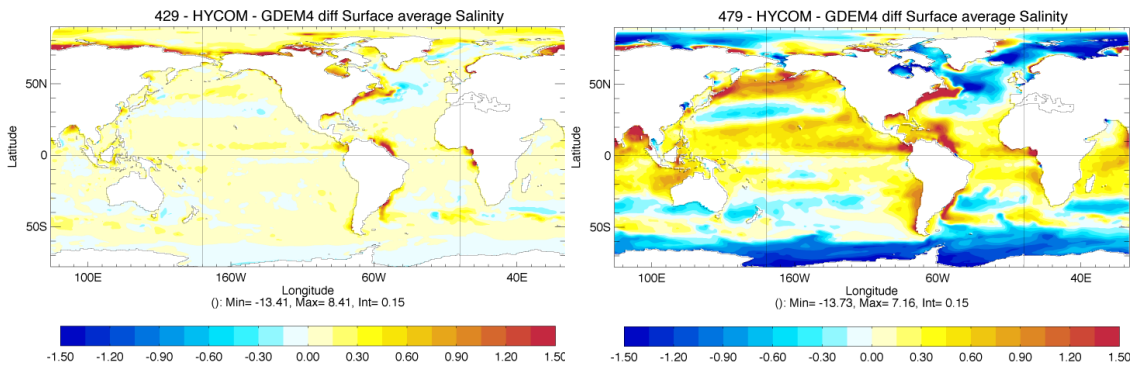


**Fig 10. Surface salinity biases after 30 years for SSS30d (left) and SSS4y (right).**

A large part of the bias in SSS4y was traced to the re-calculation of the ocean-ice fluxes based on solely the SST and ice-cover using the energy loan model built in HYCOM. We therefore performed another set of experiments to evaluate the impact of:

- the ocean-ice surface fluxes as provided by CICE instead of recalculating them in HYCOM via the energy loan model
- the Levitus climatology for the initial conditions and SSS relaxation instead of the GDEM4 climatology to better balance the initial ocean temperature with the COREv2 atmospheric heat fluxes and consequently improve the global temperature drift.

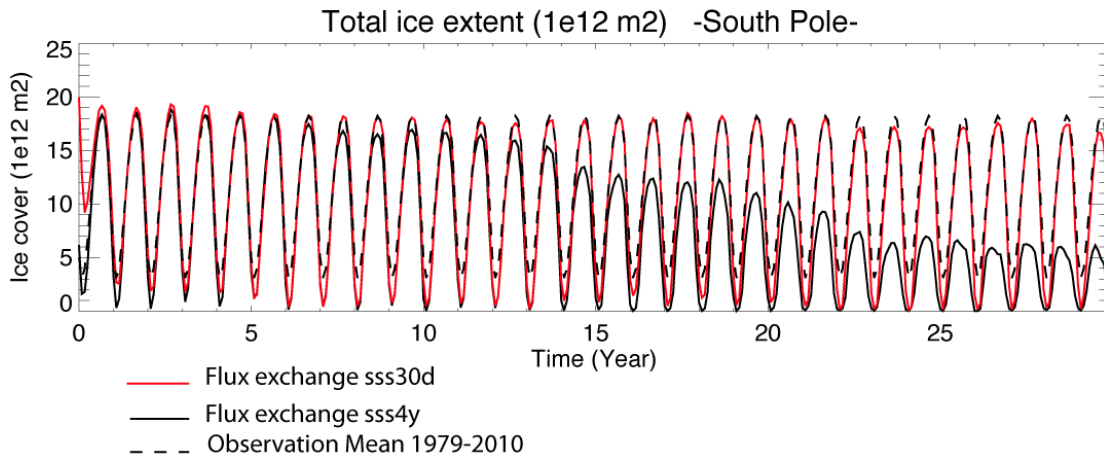


**Fig 11: Evolution of the southern pole ice extent ( $10^{12} \text{ m}^2$ ) from NSIDC-SSMI (obs.) in dashed black, CICE-SSS30d in red and CICE-SSS4y in black.**

First, we performed a new 60-year simulation keeping the SSS relaxation strong at 30 days (CICE-SSS30d), but with the ocean-ice fluxes exchanged between HYCOM and CICE and initialized from the Levitus climatology. Results are similar to SSS30d with a slight decrease of the global temperature trend ( $+0.17^\circ\text{C}$  instead of  $+0.23^\circ\text{C}$ ; Fig. 9). Decreasing the SSS relaxation to 4years/50m (CICE-SSS4y) leads to a salty bias over the poles that contributes to a strong AMOC but to the detriment of ice formation at the southern pole after 15 years (Fig 11). A spatially varying SSS relaxation was implemented with a stronger relaxation (6 months/50m) to the Southern Ocean region. The CICE-varyingSSS experiment is able to sustain an ice sheet at the South Pole for the whole 60 years of simulation with the global temperature stabilizing after 20 year around  $3.70^\circ\text{C}$  (Fig. 9 top). The maximum strength of the AMOC at  $26.5^\circ\text{N}$  for this last simulation reaches now 12.5 Sv at the end of the 1<sup>st</sup> cycle (Fig. 9 bottom), within the range of most CORE simulations (Danabasoglu et al., 2013). CICE-varying has been carried out for the full length of the CORE protocol (5 cycles) and shows a stabilization of the global temperature at  $3.71^\circ\text{C}$ , exhibits a positive bias of salt in the Arctic ( $\sim 1\text{psu}$ ), a sustained ice sheet on both Poles, but a strong variability of the strength of the AMOC. However, the CICE-varyingSSS presents a maximum AMOC of 14 Sv average over the last 20 years of the last cycle, well within the average of the other CORE-II models (Danabasoglu et al., 2013). The model outputs have been submitted to several teams of the CORE-II project and we are working on several papers to be published in peer-review journals. All experiments have been carried out on the NAVY computers Einstein and Kilrain.

## IMPACT/APPLICATIONS

The  $1/25^\circ$  (3.5 km mid-latitude) resolution, first used in some FY09 global HYCOM simulations, is the highest so far for a global ocean model with high vertical resolution. A global ocean prediction system, based on  $1/25^\circ$  global HYCOM with tides, is planned for real-time operation starting in 2015. At this resolution, a global ocean prediction system can directly provide boundary conditions to nested relocatable models with  $\sim 1$  km resolution anywhere in the world, a goal for operational ocean prediction at NAVOCEANO. Internal tides and other internal waves can have a large impact on acoustic propagation and transmission loss (Chin-Bing et al., 2003, Warn-Varnas et al., 2003, 2007), which in turn significantly impacts Navy anti-submarine warfare and surveillance capabilities. At present, regional and coastal models often include tidal forcing but internal tides are not included in their open boundary conditions. By including tidal forcing and assimilation in a fully 3-D global ocean model we will provide an internal tide capability everywhere, and allow nested models to include internal tides at their open boundaries.

## TRANSITIONS

None.

## RELATED PROJECTS

The computational effort is supported by DoD HPC Challenge and non-challenge grants of computer time.

## HONORS

Florida State University Distinguished Research Professor

## REFERENCES

- Bleck, R., 2002: An oceanic general circulation model framed in hybrid isopycnic-cartesian coordinates. *Ocean Modelling*, 4, 55-88.
- Carnes, M., R.W. Helber, C.N. Barron, and J.M. Dastugue, 2010. Validation test report for GDEM4, Technical Report NRL, Stennis, MS, 66p.
- Chassignet, E.P., L.T. Smith, G.R. Halliwell, and R. Bleck, 2003: North Atlantic simulations with the HYbrid Coordinate Ocean Model (HYCOM): Impact of the vertical coordinate choice, reference density, and thermobaricity. *J. Phys. Oceanogr.*, **33**, 2504-2526.
- Chassignet, E.P., H.E. Hurlburt, E.J. Metzger, O.M. Smedstad, J. Cummings, G.R. Halliwell, R. Bleck, R. Baraille, A.J. Wallcraft, C. Lozano, H.L. Tolman, A. Srinivasan, S. Hankin, P. Cornillon, R. Weisberg, A. Barth, R. He, F. Werner, and J. Wilkin, 2009. U.S. GODAE: Global Ocean Prediction with the HYbrid Coordinate Ocean Model (HYCOM). *Oceanography*, 22(2), 64-75.
- Cunningham, S. A., et al., 2007. Temporal variability of the Atlantic meridional overturning circulation at  $26.5^\circ\text{N}$ , *Science*, 317, 935-938, doi:10.1126/science.1141304.
- Hakkinen, S., and P. B. Rhines, 2013. Northern North Atlantic sea-surface height and ocean heat content variability, *J. Geophys. Res.*, in press.

- Halliwell, Jr., G.R., 2004: Evaluation of vertical coordinate and vertical mixing algorithms in the HYbrid-Coordinate Ocean Model (HYCOM). *Ocean Modelling*, 7, 285-322.
- Hunke, E.C. and W.H. Lipscomb, 2004. CICE: the Los Alamos sea ice model documentation and software user's manual. <http://climate.lanl.gov/Models/CICE>
- Johns, W. E., L. M. Beal, M. O. Baringer, J. R. Molina, S. A. Cunningham, T. Kanzow, and D. Rayner, 2008. Variability of shallow and deep western boundary currents of the Bahamas during 2004-05: Results from the 26°N RAPID-MOC Array, *J. Phys. Oceanogr.*, 38, 605-623, doi:10.1175/2007JPO3791.1.
- Johns, W. E., et al., 2011. Continuous, array-based estimates of Atlantic Ocean heat transport at 26.5°N, *J. Clim.*, 24 (10), 2429-2449, doi:10.1175/2010JCLI3997.1.
- Kanzow, T., et al., 2007. Observed flow compensation associated with the MOC at 26.5°N in the Atlantic, *Science*, 317, 938-941.
- Kanzow, T., et al., 2010. Seasonal variability of the Atlantic meridional overturning circulation at 26.5°N, *Journal of Climate*, 23 (21), 5678-5698, doi:10.1175/2010JCL13389.1.
- Large, W.G., and S.G. Yeager, 2009. The global climatology of an interannually varying air-sea flux data set, *Clim. Dyn.*, 33, 341-364.
- McCarthy, G., et al., 2012. Observed interannual variability of the Atlantic meridional overturning circulation at 26.5°N, *Geophys. Res. Lett.*, 39 (19), doi: 10.1029/2012GL052933.
- Rayner, D., et al., 2011. Monitoring the Atlantic meridional overturning circulation, *Deep Sea Res., Part II*, 58 (17), 1744-1753, doi:10.1016/j.dsr2.2010.10.056.5
- Richardson, P. L., and D. Walsh, 1986. Mapping climatological seasonal variations of surface currents in the tropical Atlantic using ship drifts, *J. Geophys. Res.*, 91 (C9), 10,537-10,550.
- Rosmond, T., J. Teixeira, M. Peng, T. Hogan, and R. Pauley, 2002. Navy Operational Global Atmospheric Prediction System (NOGAPS): Forcing for ocean models, *Oceanography*, 15 (1), 99-108.
- Uppala, S. M., et al., 2005. The ERA-40 re-analysis, *Quart. J. R. Meteorol. Soc.*, 131, 2961-3012, doi:10.1256/qj.04.176.
- Xu, X., W. J. Schmitz Jr., H. E. Hurlburt, and P. J. Hogan, 2012. Mean Atlantic meridional overturning circulation across 26.5°N from eddy-resolving simulations compared to observations, *J. Geophys. Res.*, 117, C03042, doi:10.1029/2010JC007586.6

## **PUBLICATIONS (2012-2013)**

- Griffies, S.M., J. Yin, P.J. Durack, P. Goddard, S.C. Bates, E. Behrens, M. Bentsen, D. Bi, A. Biastoch, C. Böning, A. Bozec, E.P. Chassignet, G. Danabasoglu, S. Danilov, C. Domingues, H. Drange, R. Farneti, E. Fernandez, R.J. Greatbatch, D.M. Holland, M. Ilicak, J. Lu, S.J. Marsland, A. Mishra, K. Lorabacher, A.J.G. Nurser, D. Salas y Méliá, J.B. Palter, B.L. Samuels, J. Schröter, F.U. Schwarzkopf, D. Sidorenko, A.-M. Treguier, Y. Tseng, H. Tsujino, P. Uotila, S. Valcke, A. Aurore, Q. Wang, M. Winton, and X. Zhang, 2013. An assessment of global and regional sea level for years 1993-2007 in a suite of interannual CORE-II simulations. *Ocean Modelling*, submitted.

- Todd, A.C., S.L. Morey, and E.P. Chassignet, 2013. Circulation dynamics and cross-shelf transport mechanisms in the Florida Big Bend, *J. Mar. Res.*, submitted.
- Danabasoglu, G., S.G. Yeager, D. Bailey, E. Behrens, M. Bentsen, D. Bi, A. Biastoch, C. Böning, A. Bozec, V.M. Canuto, C.e Cassou, E.P. Chassignet, A.C. Coward, S. Danilov, N. Diansky, H. Drange, R. Farneti, E. Fernandez, P.G. Fogli, G. Forget, Y. Fujii, S.M. Griffies, A. Gusev, P. Heimbach, A. Howard, T. Jung, M. Kelley, W.G. Large, A. Leboissetier, J. Lu, G. Madec, S.J. Marsland, S. Masina, A. Navarra, A.J.G. Nurser, A. Pirani, D. Salas y Mélia, B.L. Samuels, M. Scheinert, D. Sidorenko, A.-M. Treguier, H. Tsujino, P. Uotila, S. Valcke, A. Voldoire, Q. Wang, 2013. North Atlantic simulations in Coordinated Ocean-ice Reference Experiments phase II (CORE-II). Part I: Mean states. *Ocean Modelling*, in press.
- Yan, Y., E.P. Chassignet, Y. Qi, and W.K. Dewar, 2013. Freshening of subsurface waters in the Northwest Pacific subtropical gyres: Observations and dynamics. *J. Phys. Oceanogr.*, in press.
- Michael, J.-P., V. Misra, E.P. Chassignet, 2013: The El Niño Southern Oscillation in the historical centennial integrations of the new generation of climate models. *Reg. Environ. Change*, **13**, (Suppl. 1) S121-S130, doi:10.1007/s10113-013-0452-4.
- Winterbottom, H.R., E.W. Uhlhorn and E.P. Chassignet, 2012. A design and an application of a regional coupled atmosphere-ocean model for tropical cyclone prediction. *J. Adv. Model. Earth Syst.*, **4**, M10002, doi:10.1029/2012MS000172.
- Misra, V., J.-P. Michael, R. Boyles, E.P. Chassignet, M. Griffin, and J.J. O'Brien, 2012. Reconciling temperature trends in the Southeast United States. *J. Climate*, doi:10.1175/JCLI-D-11-00170.1.
- Chassignet, E.P., C. Cenedese, and J. Verron (Eds.), 2012. *Buoyancy-Driven Flows*. Cambridge University Press, 436 pp.